Energy Management System for Microgrids Including Batteries with Degradation Costs

Chengquan Ju, *Student Member, IEEE*, and Peng Wang, *Senior Member, IEEE*

***Abstract*—Integration of renewable energy source (RES) and energy storage system (ESS) in microgrids has a potential benefit to users and system operators. However, new operating issues brought by RES and high cost of ESS need to be scrutinized for economic operation of microgrids. In order to evaluate the economic operation, this paper presents a predictive energy management system (EMS) for microgrids that manifests the process of battery degradation under the minimum system operating cost. The proposed EMS provides the power dispatch based on the hourly-ahead price and forecast data in a most cost-saving way, in which the battery degradation cost with respect to the depth of charge and lifetime is incorporated, transforming the long-term installation cost to the short-term operational cost that accounts for the real-time scheduling. The effectiveness of the proposed method is illustrated by case studies in the simulation.**

***Keywords*—Energy storage; energy management system; model predictive control (MPC); microgrids; optimization.**

I. Introduction

The rapid development of renewable energy techniques has prompted microgrids to change towards more intelligent and more efficient entities. Microgrid is defined as a cluster of distributed generation units and energy storages and is able to supply power to local users in a decentralized manner [1]. However, variability of renewable energy system (RES) induces stability issues. In particular, renewables may not provide enough energy when electricity is heavily needed [2]. Energy storages are usually integrated to compensate power intermittency. Energy storages can also act as bidirectional mediators with the utility grid (UG) to provide financial benefits for the users based on various strategies.

Unlike large-scale systems which usually have abundant reserves, the operating reserve is often provided by batteries in microgrids. Increasing the operating reserve can reduce the probability of loss of load and thus increase the system reliability [3], however, high capital cost of batteries may bring unexpected cost, making the system become less economic [4]. To this end, studies have been featured on the design of energy management system (EMS) of microgrids for unpredictable variation by RES and efficient operation of batteries [5]. Research in [6] decomposes the energy management problem in a microgrid into a unit commitment problem for voltage and frequency regulation and an optimal power flow problem for reactive power support. In [7], charging and discharging events of batteries are determined by heuristic methods with a centralized EMS and local EMSs at user sides. Research focusing on batteries in microgrids varies from real-time operations addressing instant power sharing [8, 9] and frequency regulation [10] to scheduling problems manifesting charging strategies [11] and optimization in the long term [12, 13]. However, few of the above studies has investigated effects of the degradation process of batteries, leading to gross error on the scheduling problems and even brings unexpected failures. Further, inconsideration on influences of different characteristics of batteries on the structure of EMS exists in literature.

In view of the above challenges, appropriate methods need to be developed so that the economic operation and system reliability must be spontaneously scrutinized. The first contribution of this paper is that the battery degradation cost model considering the main characteristics is devised. It features a practical connection on the installation cost in the long term and economic dispatch problem in the short term. The second contribution is the development of a predictive EMS based on nonlinear MPC that not only matches the power balance in a most cost-saving way but also accounts for the battery degradation process. The remainder of the paper is organized as follows. In Section II, the system model of a general microgrid structure is presented, and the battery degradation cost model considering lifetime and DOD is discussed. Section III is focused on the formulation of the proposed predictive EMS. Case studies and results are presented in Section IV. At last, the relevant conclusion and the contribution of the paper is highlighted.

II. System Modelling

Without loss of generality, we consider a microgrid which is comprised of the point of common coupling (PCC) to the UG, a battery, a RES system and the aggregated load as shown in Fig. 1. Practically, the microgrid can operate in connection with the UG or independently, depending on system requirements of operators, the sizing of RES and load demand. The main objective of the control strategy is to keep power balance in order to maintain system stability when operating in the isolated mode. When in the grid-connected mode, the microgrid can maximize the user benefits by purchasing and selling electricity with the UG. In this context, the EMS in the microgrid is required to allocate the energy source in an economic way. We will focus on the grid connected mode in the following discussion unless specified otherwise.

A. PCC and Electricity Price

The price of electricity supplied from the UG is usually determined by the upper-level system operator in a static or

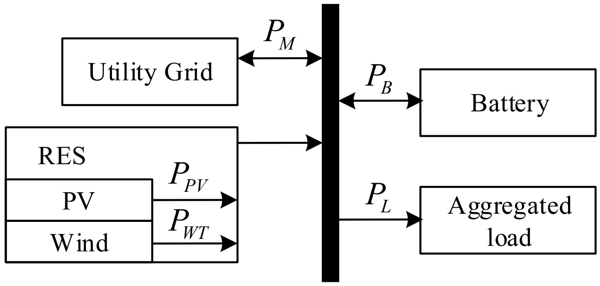

Fig. 1. System model of the microgrid.

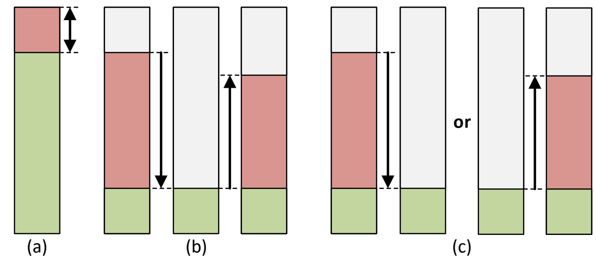

Fig. 2. Different definitions on DOD.

dynamic fashion [14]. Static pricing schemes, including fixed and time-of-use pricing, are often pre-announced in advance and do not change with network conditions. For microgrid users, fixed electricity prices do not influence user patterns since the cost does not change with the quantity of use, whereas time-of-use prices prompt more electricity to be used in off-peak hours considering relatively lower rates per *kWh*. As for dynamic pricing schemes such as real-time and on-demand pricing, they are sensitive to locational marginal prices and are often announced hours ahead [14], which allows users making advanced planning to minimize their operation costs and even selling a part of excess electricity to the UG.

In order to present general cases for the microgrid, two pricing schemes including time-of-use pricing and dynamic real-time pricing are used in this paper. In the time-of-use pricing model, we assume the electricity price as a two-level model which has an off-peak price an on-peak price. In the dynamic real-time pricing model, the half hourly price data over a year from Energy Market Company of Singapore [15] is weighted and averaged to the hourly data, starting from May 2013 to April 2014. Moreover, the selling price is also set in both pricing models, indicating the price per *kWh* that the microgrid sell extra generation back to the UG, which is lower than the buying price.

B. Forecast error on RES

The implementation of RES in the microgrid gives the energy management a more cumbersome task to track the instantaneous load. The microgrid is modelled with two RES systems including PV panels and wind turbines. PV generation is considered to have great variation due to the passing clouds. Wind power is closely correlated with wind speed, which has different patterns on seasons and even days. The forecast error of RES is considered to have a close relationship with the prediction time. Solar power ranges from 20% to 35% root mean square (RMS) error depending on different irradiance forecast techniques. Day-ahead wind forecast error currently averages at more than 10% RMS error of the capacity, and progressively reduces half to 5%-6% for an hour-ahead forecast [16]. Following this idea, the RES output in this paper is modelled to have a gradient uncertainty level, in which the forecast error increases as the prediction horizon becomes larger. There are also many ongoing studies on forecasting methodologies of RES, however, since it is outside the scope of this paper, the analysis of performance of different forecasting techniques will not be further discussed.

C. Battery Degradation Cost

Battery is considered to have good performance on power density and energy density, thus it can be scheduled as distributed generation unit to maintain the instantaneous power balance of the system and minimize the operating cost in a long period of time. The degradation on battery lifetime mainly features on two factors, namely, the aging of cycle life that reflects the total achievable cycle count of a battery, and the capacity wear that accounts for the usable energy [17]. Cycling conditions, such as the number of frequent charging and discharging, charging and discharging rates and maintenance schedules, have a great effect on the battery lifetime which may cease to failure due to accelerated degradation by daily usage. Even if under proper maintenance and not in use, batteries would still suffer from certain degree of aging. Apart from cycling conditions, state parameters also have significant influences on battery lifetime [18]. Excessive high or low state of charge (SOC) would deteriorate battery charging and discharging performance. Temperature may have a negative impact on the battery life as well, that at high temperatures the decay process will be accelerated. In practical, the temperature controller is often included in the battery management system. Therefore, it is assumed that the battery degradation due to ambient factors can be neglected. As for the effect of charging rate, its direct impact on battery lifetime is negligible in comparison of other parameters when battery is operating within a certain degree of rated current [19].

Based on the above assumptions, the primary determinants on battery lifetime are the actual full capacity and the depth of discharge (DOD). There are two general DOD definitions in the literature in accordance with different cycling events as shown in Fig. 2(a) and (b). The first is the discharged energy from the full capacity (100% SOC), and the second refers to a full cycle consisting of one charging and discharging event [20]. Unless other specified in this paper, SOC is defined as the leftover energy compared to the full capacity, and DOD is defined as the energy in the half cycle of one charging or discharging event with respect to the full capacity [20], as illustrated in Fig. 2(c). We also define the actual full capacity of the battery to be the amount of energy that can be stored at 100% SOC. Note that a cycle event is counted whenever the operating modes (charging and discharging) switch to the opposite sides.

Fig. 3 shows a relationship between the number of life cycles and the DOD of Ni-Cd batteries [19]. The battery lifetime has the best fitting in the following expression with the DOD:

$$L_B(d_B) = a \times d_B^{\,-b} \times e^{-cd_B} \tag{1}$$

where $a, b, c > 0$ are curve-fitting coefficients. As expected, the number of life cycles decreases with the increasing DOD. Without loss of generality, this expression is also applied for other types of batteries with different parameters such as Lithium-Ion and Lead-Acid batteries [21]. The statistical data is identified and provided by manufacturing specifications, however, it should be noted that all charging and discharging cycles in the statistical data are assumed to be under conditions with constant DOD, which is apparently impractical because the batteries are always cycled at various levels of DOD in real-time operation. Therefore, estimation of battery degradation cost by using the above information would introduce gross errors. To the best of our knowledge, however, there is unfortunately no existing work featuring on direct relationships of variable DODs and battery lifetime. Therefore, in order to take the battery degradation cost model in a practical fashion, it is reasonably assumed that the empirical data of life cycles is accurate enough to estimate the long-term degradation effect, in other words, the effect of each charging and discharging cycle event on the lifetime is irrelevant with the historical charging and discharging profiles.

Given the actual capacity and DOD as two factors, the battery degradation model is based on the following premises:

a) The degradation process is considered to be time-linear throughout the whole battery life; and

b) The degradation cost of each charging and discharging cycle event with the same level of DOD is the same at different levels of SOC.

It is noted that operation at too high or low SOC for too long time would in fact rise the internal impedance and decompose electrolyte in the battery, leading to capacity loss and power fade, however such fade in a short term would be insignificant compared with the degradation caused by chronic charging and discharging events.

The battery degradation cost model represents a direct depreciation on its actual capacity and lifetime. Consider a discharging event starting at time $t{=}t_0$ with the average power $P_B(t)$ for a time interval Δt, the DOD of the battery can be presented as:

$$d_B(t_0) = \frac{P_B(t_0)\Delta t}{E_B(t_0)} \tag{2}$$

where $E_B(t_0)$ is the real-time actual capacity at $t{=}t_0$. Considering the charging/discharging efficiency coefficients η_c and η_d, the average degradation cost per unit energy in this event according to Fig. 1 can be formulated as follows [22]:

$$C_{BAC}\left(t_0, d_B(t_0)\right) = \frac{C_B \Delta t}{2L_B(d_B)E_B(t_0)d_B(t_0)\eta_{Bc}\eta_{Bd}} \tag{3}$$

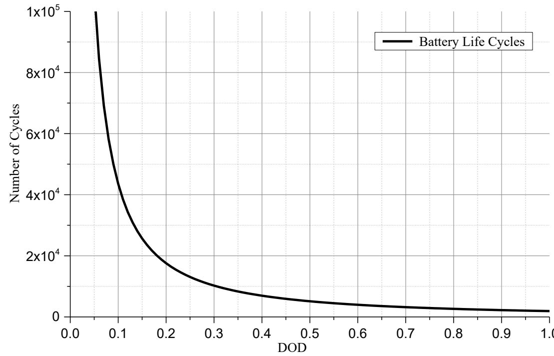

Fig. 3. Relationship of number of lifecycles and DOD of Ni-Cd battery.

Note that it is a levelized degradation cost for each charging and discharging event at DOD=d_B. Therefore, we can get the corresponding battery degradation cost for this discharging event by simply multiplying the energy exported from the battery:

$$\begin{aligned} C_{BDC}\left(t_0, d_B(t_0)\right) &= C_{BAC}\left(t_0, d_B(t_0)\right) P_B(t_0) \\ &= \frac{C_B P_B(t_0)\Delta t}{2L_B\left(d_B(t_0)\right)E_B(t_0)d_B(t_0)\eta_{Bc}\eta_{Bd}} \end{aligned} \tag{4}$$

The actual capacity of the battery should be deprecated for a certain amount after each cycle event. The actual capacity of the battery at $t{=}t_0{+}\Delta t$ can be recalculated as:

$$E_B(t_0 + \Delta t) = E_B(t_0) - \frac{E_{B.rated}}{L_B\left(d_B(t_0)\right)} \tag{5}$$

where $E_{B.rated}$ is the rated battery capacity. As for the charging event, the cost is equal as if the battery is discharging, specifying an equal degradation effect on the battery. Note that the effect of the charging and discharging rate on the battery life will not be considered as a long-term effect, as long as its current does not exceed the limit defined by manufacturer specifications. Similar situations will not be further discussed for other external parameters such as ambient temperature and maintenance [22].

III. Formulation of The Optimization Problem

A. Problem Statement

The proposed predictive energy management strategy aims to optimize the power dispatch for a finite period of time in order to achieve the minimal operational cost in the microgrid. We consider a discrete-time system which consists of a nonlinear MPC with a receding time horizon $t \in T$. The total operational cost of the microgrid which includes the electricity price of the UG and the battery degradation cost. The management strategy firstly makes the scheduling over the whole horizon T based on the forecast data including electricity prices, loads and renewable outputs. By using forecast data, all future control actions within T can be required, however only solutions within the first time interval will be utilized. Then, the EMS updates state variables from solutions and starts the scheduling for the next time interval.

B. Dynamics and Constraints

In practical, State dynamics must be specified for the battery in terms of capacities and charging/discharging power at all times. Let $P_B(t)$ denote the output power of battery. With charging and discharging efficiencies, the discrete-time difference equation on the capacity change can be presented as follows:

$$E_B(t)=\begin{cases} E_B(t-1)+P_B(t)\Delta t\eta_{Bc}, \; P_B(t)\le 0 \\ E_B(t-1)+\dfrac{P_B(t)\Delta t}{\eta_{Bd}}, \quad P_B(t)>0 \end{cases}, \quad t\in T \tag{6}$$

Note that the negative output means the battery is charging.

Several constraints should be meet as well. First, the power balance must be satisfied at all times, which can be formulated as follows:

$$P_L(t)=P_M(t)+P_B(t)+P_{PV}(t)+P_{WT}(t),\; t\in T \tag{7}$$

The inequality constraints include physical limitations on the power of the UG and the battery. These constraints can be presented as follows, respectively:

$$P_M^{\min}(t)\le P_M(t)\le P_M^{\max}(t), \quad t\in T \tag{8}$$

$$P_B^{\min}\left(t\right)\le P_B\left(t\right)\le P_B^{\max}\left(t\right) \quad ,t\in T \tag{9}$$

Note that when a bidirectional communication is allowed, the lower boundary is negative because the microgrid can sell electricity back the UG.

In addition, the capacity limits of the battery can be written as follows:

$$E_B^{\min}(t)<E_B(t)<E_B^{\max}(t), \quad t\in T \tag{10}$$

C. Problem Formulation

The objective function manifests the operational cost of the microgrid, which includes the electricity price from the UG and the battery degradation cost within a predefined timeframe. The mathematical formulation can be written as follows:

$$F:\ \min\left(\sum_{t=1}^{T}C_M(t)+\sum_{t=1}^{T}C_B(t)\right) \tag{11}$$

In the above equation, the first term represents the electricity cost in connection with the UG, which can be expressed as:

$$C_M(t)=c_m(t)\times P_M(t) \tag{12}$$

The second term describes the battery degradation cost. Here, we denote $g(t)$ as the state flag to indicate the transition on the charging and discharging modes in consecutive time intervals, and $E_a(t)$ as the accumulative energy in kWh before the operating mode of battery has been changed. $g(t)$ can be described by the following equation:

$$g(t)=\begin{cases} 1, & if\ P_B(t)\times P_B(t-1)\le 0 \\ 0, & if\ P_B(t)\times P_B(t-1)>0 \end{cases} \tag{13}$$

Correspondingly, we can get accumulative energy calculated as

$$E_a(t)=\begin{cases} E_a(t-1)+P_B(t)\times\Delta t, if\ g(t)=0 \\ P_B(t)\times\Delta t, \qquad\qquad if\ g(t)=1 \end{cases} \tag{14}$$

Using $E_a(t)$ in consecutive time intervals, the battery degradation cost can be derived as in the following expression:

$$C_B(t)=\begin{cases} C_{DC}(t,\dfrac{g(t)}{E_B(t)})-C_{DC}(t,\dfrac{g(t-1)}{E_B(t-1)}), if\ E_a(t)=0 \\ C_{DC}(t,\dfrac{g(t)}{E_B(t)}), \qquad\qquad if\ E_a(t)=1 \end{cases} \tag{15}$$

Thus, the formulation of the optimization problem can be expressed as follows:

$$\begin{gathered} F:\ \min\left(\sum_{t=1}^{T}C_M(t)+\sum_{t=1}^{T}C_B(t)\right) \\ s.t.\ (5)\sim(9),(12)\sim(15) \end{gathered} \tag{16}$$

IV. Case Studies

In this section, case studies under different scenarios are conducted to demonstrate the proposed predictive EMS with battery degradation cost. The simulation is conducted for a 48h horizon and the time interval is set to be 1h. The forecast error associated with RES is adopted with the standard deviation from 10% to 40% at the time terminal of the predictive horizon.

A. Case 1: Pricing Schemes

In case 1, two types of pricing schemes including time-of-use pricing and real-time pricing are considered in different scenarios. In the time-of-use pricing, the electricity price is set as 0.1$/kWh during off-peak hours (hour 0-8 and 18-23) and 0.25$/kWh at on-peak hours (hour 9-17). In the real-time pricing, the hourly data is adopted by weighting the half hourly data from May 2013 to April 2014 in Energy Market Company of Singapore [15]. We also determine the selling price as 80% of the electricity price both pricing schemes. To make a comparison, we also conduct two scenarios in which no battery degradation cost will be considered in the formulation. However, the cost due to charging and discharging losses will be added instead.

Results of the optimal dispatch of all scenarios are shown in Fig. 4. As expected, in the time-of-use pricing scheme, the battery operation is mainly scheduled by the electricity price that the battery is charging during off-peak hours and discharging during on-peak hours as seen in Fig 4(a) and (b). In addition, when the battery degradation cost is implemented, excessive energy generated by the RES from hour 10 to 13 is sold back to the UG. In the real-time pricing scheme, similar results can be also illustrated that the battery has more sensitive responses to high electricity prices at hour 11 and 16 when the battery is quickly discharged. When the electricity price is

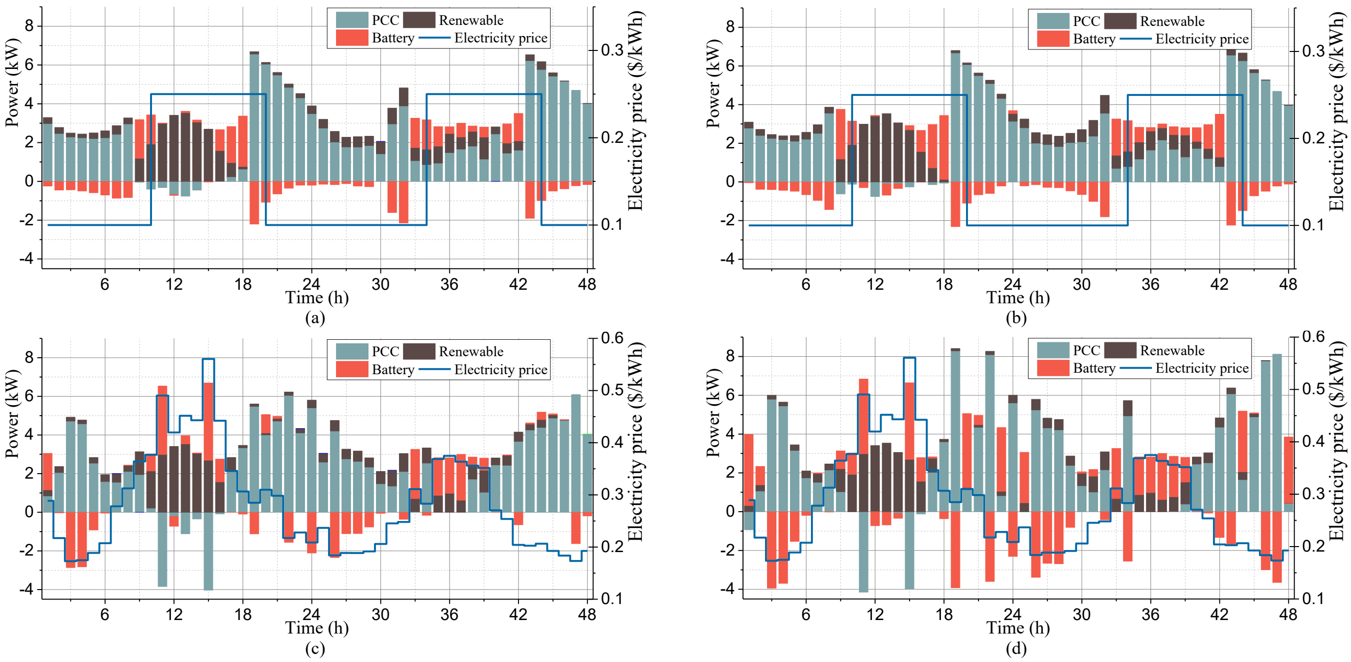

Fig. 4 Case 1: optimal dispatch in all scenarios which include: (a) time-of-use pricing with degradation cost; (b) time-of-use without degradation cost; (c) real-time pricing with degradation cost; and (b) real-time pricing without degradation cost.

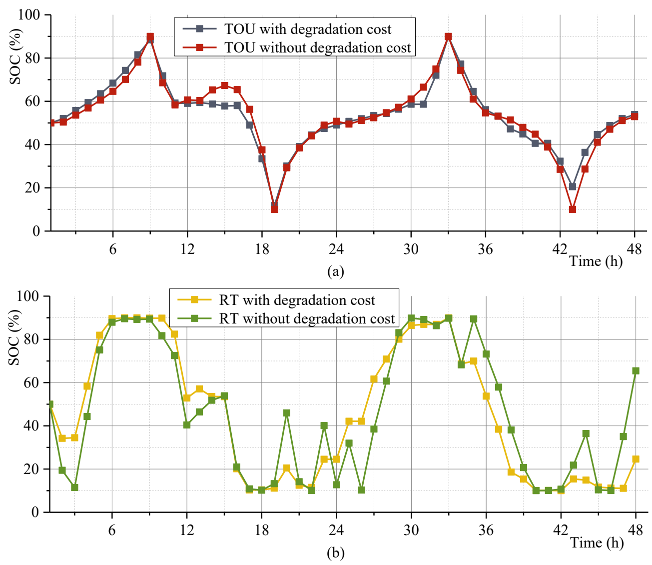

Fig. 5. Case 1: hourly average cost in: (a) the time-of-use pricing scheme; and (b) the real-time pricing scheme.

relatively low from hour 16 to 32, as shown in Fig. 4(c), the battery is charged to ensure enough energy can be discharged in next following hours.

By comparing the dispatch strategies with and without the implementation of the battery degradation cost, it can be also observed in Fig. 4 that the battery is frequently cycled without the degradation cost. Fig. 5 shows the SOC changes in all scenarios that the scheduling without the degradation cost results into large variations on cycling events, which is not beneficial for the battery life.

The average hourly operational operational cost and the

TABLE 1. Average hourly operational and degradation cost in all scenarios.

Scenario	Operational cost ($)	Battery degradation cost ($)
TOU with degradation cost	**0.2955**	**0.0176**
TOU without degradation cost	0.2982	0.0264
RT with degradation cost	**0.5118**	**0.0209**
RT without degradation cost	0.5349	0.0540

battery degradation cost in all scenarios are presented in Table 1. It shows that the operation cost and battery degradation cost have been both significantly decreased when the degradation process of battery has been considered into the formulation. Note that the battery degradation cost is calculated based on the operation scheduling even in scenarios which do not include the formulation of the degradation cost.

B. Case 2: Prediction Horizon

In case 2, we consider six time lengths of prediction horizon from 6h to 96h to show the effects on the operational strategies, respectively. In addition, we adopt the time-of-use pricing scheme for all the scenarios.

The SOC of the battery in 48 hours with different prediction horizons is depicted in Fig. 6(a). It is observed that the optimal operation scheduling of battery is influenced much when the prediction horizon is low, however when it reaches a certain degree (24h), the SOC change becomes much less significant. The operational cost and the battery degradation cost are shown in Fig. 6 (b) and (c), which shares very similar changing patterns that high levels of details on prediction horizon provides less variation on costs. However, it is shown in Fig. 6(d) that despite of the length of prediction horizon, the total operation cost in 48 hours does not have great variations, while

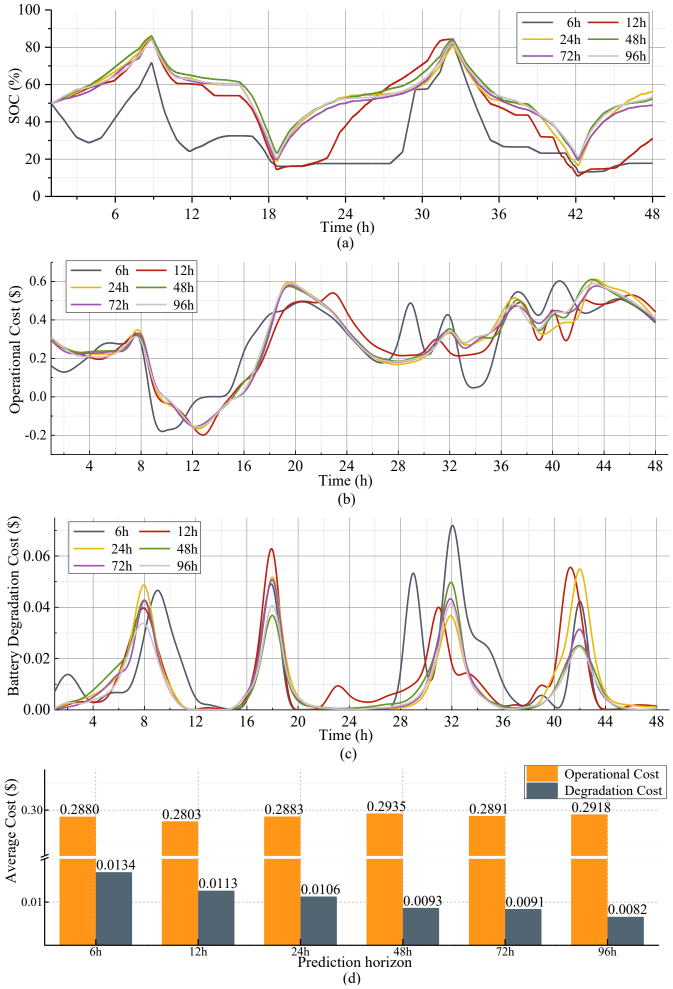

Fig. 6. Case 2: (a) SOC of battery; (b) operation cost; (c) battery degradation cost; and (d) average hourly cost with different prediction horizons.

a significant decrease on the battery degradation cost has taken place with the increasing prediction horizon.

V. Conclusion

In this paper, we proposed a predictive EMS in a microgrid with the battery considering its degradation cost. We addressed the optimization problem in the way that the minimization of the operational cost of the microgrid can be achieved. The battery degradation cost model was introduced to feature the long-term installation cost into short-term scheduling problems. Following the battery degradation cost model, the predictive EMS is developed, in which the total operational cost of the microgrid is minimized in a finite time horizon. The proposed EMS is applied to a microgrid which includes the PCC to the UG, the battery, a RES system and aggregated load, and the effectiveness of the proposed EMS is illustrated by case studies.

References

[1] K. Rahbar, X. Jie, and Z. Rui, "Real-Time Energy Storage Management for Renewable Integration in Microgrid: An Off-Line Optimization Approach," IEEE Trans. Smart Grid, vol. 6, pp. 124-134, 2015.

[2] A. Tani, M. B. Camara, and B. Dakyo, "Energy Management in the Decentralized Generation Systems Based on Renewable Energy—Ultracapacitors and Battery to Compensate the Wind/Load Power Fluctuations," IEEE Trans. Ind. Applicat., vol. 51, pp. 1817-1827, 2015.

[3] M. Q. Wang and H. B. Gooi, "Spinning Reserve Estimation in Microgrids," Ieee T Power Syst, vol. 26, pp. 1164-1174, 2011.

[4] K. Worthmann, C. M. Kellett, P. Braun, L. Grune, and S. R. Weller, "Distributed and Decentralized Control of Residential Energy Systems Incorporating Battery Storage," IEEE Trans. Smart Grid, vol. 6, pp. 1914-1923, 2015.

[5] M. Yazdanian and A. Mehrizi-Sani, "Distributed Control Techniques in Microgrids," IEEE Trans. Smart Grid, vol. 5, pp. 2901-2909, 2014.

[6] D. E. Olivares, Can, x, C. A. izares, and M. Kazerani, "A Centralized Energy Management System for Isolated Microgrids," IEEE Trans. Smart Grid, vol. 5, pp. 1864-1875, 2014.

[7] H. Kanchev, L. Di, F. Colas, V. Lazarov, and B. Francois, "Energy Management and Operational Planning of a Microgrid With a PV-Based Active Generator for Smart Grid Applications," IEEE Trans. Ind. Electron., vol. 58, pp. 4583-4592, 2011.

[8] J. Shen and A. Khaligh, "A Supervisory Energy Management Control Strategy in a Battery/Ultracapacitor Hybrid Energy Storage System," IEEE Trans. Transport. Electrific, vol. 1, pp. 223-231, 2015.

[9] J. Xiao, P. Wang, and L. Setyawan, "Hierarchical Control of Hybrid Energy Storage System in DC Microgrids," IEEE Trans. Ind. Electron., vol. 62, pp. 4915-4924, 2015.

[10] N. Mendis, K. M. Muttaqi, and S. Perera, "Management of Battery-Supercapacitor Hybrid Energy Storage and Synchronous Condenser for Isolated Operation of PMSG Based Variable-Speed Wind Turbine Generating Systems," IEEE Trans. Smart Grid, vol. 5, pp. 944-953, 2014.

[11] Q. Xie, Y. Wang, Y. Kim, M. Pedram, and N. Chang, "Charge Allocation in Hybrid Electrical Energy Storage Systems," IEEE Trans. Computer-Aided Design, vol. 32, pp. 1003-1016, 2013.

[12] Y. Ghiassi-Farrokhfal, C. Rosenberg, S. Keshav, and M. B. Adjaho, "Joint Optimal Design and Operation of Hybrid Energy Storage Systems," Ieee J Sel Area Comm, vol. 34, pp. 639-650, 2016.

[13] M. E. Choi, S. W. Kim, and S. W. Seo, "Energy Management Optimization in a Battery/Supercapacitor Hybrid Energy Storage System," IEEE Trans. Smart Grid, vol. 3, pp. 463-472, 2012.

[14] A. Fakhrazari, H. Vakilzadian, and F. F. Choobineh, "Optimal Energy Scheduling for a Smart Entity," IEEE Trans. Smart Grid, vol. 5, pp. 2919-2928, 2014.

[15] EMCSG. (2015). *Market Data*. Available: https://www.emcsg.com/marketdata

[16] P. P. Varaiya, F. F. Wu, and J. W. Bialek, "Smart Operation of Smart Grid: Risk-Limiting Dispatch," P Ieee, vol. 99, pp. 40-57, 2011.

[17] K. Smith, M. Earleywine, E. Wood, and A. Pesaran, "Battery wear from disparate duty-cycles: Opportunities for electric-drive vehicle battery health management," in American Control Conference, June 27-29, 2012, Montreal, Canada, 2012.

[18] J. Vetter, P. Novák, M. R. Wagner, C. Veit, K. C. Möller, J. O. Besenhard, et al., "Ageing mechanisms in lithium-ion batteries," J Power Sources, vol. 147, pp. 269-281, 9/9/ 2005.

[19] S. Drouilhet and B. Johnson, "A Battery Life Prediction Method for Hybrid Power Applications Preprint," 1997.

[20] M. Koller, T. Borsche, A. Ulbig, and G. Andersson, "Defining a degradation cost function for optimal control of a battery energy storage system," in PowerTech (POWERTECH), 2013 IEEE Grenoble, 2013, pp. 1-6.

[21] C. Zhou, K. Qian, M. Allan, and W. Zhou, "Modeling of the cost of EV battery wear due to V2G application in power systems," Ieee T Energy Conver, vol. 26, pp. 1041-1050, 2011.

[22] S. Han, S. Han, and H. Aki, "A practical battery wear model for electric vehicle charging applications," Appl Energ, vol. 113, pp. 1100-1108, 2014.